# A P/N/Si-containing hyperbranched flame retardant for improving mechanical performances, fire safety, and UV resistance of epoxy resins

Haonan Wang [a], Siqi Huo [b,c,*], Cheng Wang [a], Guofeng Ye [a], Qi Zhang [a], Pingan Song [c,d], Hao Wang [b,c], Zhitian Liu [a,**]

[a] Hubei Engineering Technology Research Center of Optoelectronic and New Energy Materials, School of Materials Science & Engineering, Wuhan Institute of Technology, Wuhan 430205, China
[b] School of Engineering, University of Southern Queensland, Springfield 4300, Australia
[c] Centre for Future Materials, University of Southern Queensland, Springfield 4300, Australia
[d] School of Agriculture and Environmental Science, University of Southern Queensland, Springfield 4300, Australia

## ARTICLE INFO

## ABSTRACT

The applications of epoxy resin (EP) are limited in many high-tech fields due to its unsatisfied fire safety and mechanical properties, but introducing flame retardants usually further deteriorates mechanical properties. In this work, a flame-retardant hyperbranched polymer SD was synthesized from 9, 10-dihydro-9-oxa-10-phospha-phenanthrene-10-oxide (DOPO), diethanolamine, polyformaldehyde, and phenyltrimethoxysilane (PTMS), and applied in high-performance EP. The results showed that the resultant EP-SD samples maintain high transparency and show improved UV-shielding performances. 1.5 wt% of SD allows EP to achieve a vertical burning UL-94 V-0 classification, indicative of high efficiency. EP-SD$_6$ with 6 wt% SD obtains a limiting oxygen index (LOI) of 36.0 % and its peak heat release rate (PHRR) and peak smoke release rate (PSPR) are 65.4 % and 20.2 % lower than those of the neat EP. The addition of SD also improves the mechanical properties of EP. The tensile strength, elongation at break, flexural strength and impact strength of EP-SD$_6$ are increased by 70.4 %, 68.4 %, 30.2 % and 59.7 %, respectively. The superior flame retardancy and mechanical properties of EP-SD$_6$ enable it to stand out from flame-retardant EP systems. Therefore, this work provides a rational design strategy for preparing fire-safe EPs with great optical and mechanical properties based on hyperbranched polymers, which can satisfy the requirements of different industries.

## 1. Introduction

EP, as one of the most common polymer materials, has excellent chemical resistance and adhesive properties, so it is widely used in various industries, such as electronics, electrical equipment and aerospace [1–3]. However, EP is easy to burn, and it will release toxic smoke during the combustion process, which causes great safety risks [4,5]. Therefore, it is essential to address the flammability of EP and reduce its smoke release during combustion [6]. Adding flame retardants is a simple yet effective strategy to solve the above problems [7].

Traditional halogenated flame-retardants have been widely used in the past because of their excellent flame-retardant properties, but they produce a large number of toxic and acidic fumes during combustion, seriously threatening the environment and human health. Hence, many

of them have recently been banned in different countries [8–10]. Phosphorus-based flame retardants are considered as promising alternatives due to their low toxicity and high flame-retardant efficiency [11,12]. In particular, the phosphorus-based flame retardants can act as free radical scavengers in the gas phase during combustion and promote dehydration and carbonization of the polymer matrix in the condensed phase [13,14]. For example, Zhang et al. [15] used DOPO and 1-oxy-4-hydroxymethyl-2, 6, 7-trioxy-1-phosphodichlorooctane (PEPA) as raw materials to synthesize a phosphorus-containing flame retardant (DOPO-PEPA), and their results showed that 9.1 wt% of DOPO-PEPA made EP achieve a LOI of 35.0 % and an UL-94 V-0 rating. Wu et al. [16] synthesized a phosphaphenanthrene-derived linear oligomer (DQPC-n), and 7.2 wt% of it increased the LOI value and UL-94 classification of EP to 35.8 % and V-0, respectively. However, the radical

---

trapping of phosphorus-derived flame retardants often led to increased smoke release during combustion.

Silicon-derived flame retardants are also widely applied in polymeric materials, which can form a protective silica layer on the polymer surface to inhibit heat release and smoke generation during burning [17,18]. For example, Fang et al. [18] successfully synthesized a flame retardant (TDA) containing phosphorus, nitrogen, and silicon using 1, 3, 5-triglycidyl isocyanurate, DOPO and (3-aminopropyl) triethoxysilane as raw materials. 25.0 wt% of TDA endowed EP with a LOI of 33.4 % and an UL-94 V-0 rating, with remarkable reductions in PSPR and total smoke production (TSP) in cone calorimetry test. Obviously, most of the P/Si-containing flame retardants are effective in enhancing both flame retardancy and smoke suppression of epoxy resins.

The poor toughness of epoxy resins due to their highly cross-linked network also limits their applications in some advanced engineering fields [17]. Hyperbranched polymers show great potential in the fabrication of mechanically strong and tough EPs due to their unique branched structures and intramolecular cavities [4,19]. Cheng et al. [20] synthesized a novel boron-containing hyperbranched benzoxazine (HB-B), and applied it as a curing agent in EP. The tensile strength of the obtained EP was increased by 88.5 % compared with unmodified EP. Chen et al. [21] introduced the hyperbranched polyphosphamide (HBPPA) on the surface of CNT to form a novel CNT hybrid, which respectively increased the tensile strength and impact strength of EP by 67.9 % and 71.8 % at a low addition of 2 wt%. Although many hyperbranched polymers/flame retardants have been synthesized, these additives usually suffer from low efficiencies and poor smoke suppressing and strengthening/toughening effects. Therefore, it is necessary yet challenging to develop highly-effective hyperbranched polymers with flame-retardant, smoke-suppressing, strengthening and toughening functions.

Herein, a novel phosphorus/nitrogen/silicon-containing hyperbranched flame retardant is synthesized in this work and utilized as a multifunctional flame retardant for epoxy resins. Due to the combined action of the P, N and Si elements in SD, only 1.5 wt% of it enables EP to pass an UL-94 V-0 rating, with a LOI of 29.5 %. Moreover, the introduction of SD significantly enhances the UV resistance, mechanical strength and toughness of EP. Hence, the high-performance EP-SD systems with superior fire safety, UV-shielding performances and mechanical properties show enormous potential in high-tech industries.

## 2. Material and methods

### 2.1. Materials

Diglycidyl ether of bisphenol-A (DGEBA, CYD-127, epoxide equivalent weight: ~185 g/equiv) was provided by Yueyang Baling Petrochemical Co., Ltd. (Hunan, China). Trichloromethane and anhydrous ethanol were supplied by Sinopharm Chemical Reagent Co., LTD. (Shanghai, China). 9, 10-Dihydro-9-oxa-10-phosphaphenanthrene-10-oxide (DOPO), diethanolamine, *N*, *N*-Dimethylformamide (DMF), polyformaldehyde, dichloromethane and phenyltrimethoxysilane (PTMS) were purchased from Energy Chemical Co., Ltd. (Shanghai, China).

### 2.2. Synthesis of the Si/P-containing flame retardant (SD)

The synthesis route of SD is shown in Fig. 1a. The phosphorus-based intermediate (DHDP) was synthesized based on a previous work [22]. The obtained DHDP (33.3 g), PTMS (9.9 g), and DMF (100 mL) were introduced in a flask, and continuously reacted under magnetic stirring at 120 °C for 6 h with a nitrogen flow. Most of DMF was removed by reduced-pressure distillation for 2 h at 100 °C. Then, the crude product was dried in a vacuum oven at 80 °C for 24 h to obtain the final solid SD.

### 2.3. Preparation of EP samples

The proportions of each component of EP samples are shown in Table S1. The EP samples were prepared as follows. SD was dissolved in dichloromethane (the ratio of SD to dichloromethane = 1 g: 5 mL), and then DGEBA was added and mechanically stirred at 40 °C until being transparent. The solution was heated to 80 °C and stirred for 2 h to remove dichloromethane. DDM was then added and stirred rapidly for 10 min. After vacuum defoamation for 3 min, the solution was transferred to a preheated stainless-steel mold at 80 °C. It was cured at 80 °C for 2 h and at 150 °C for 4 h. The neat EP was prepared based on the above method without adding SD.

### 2.4. Characterizations

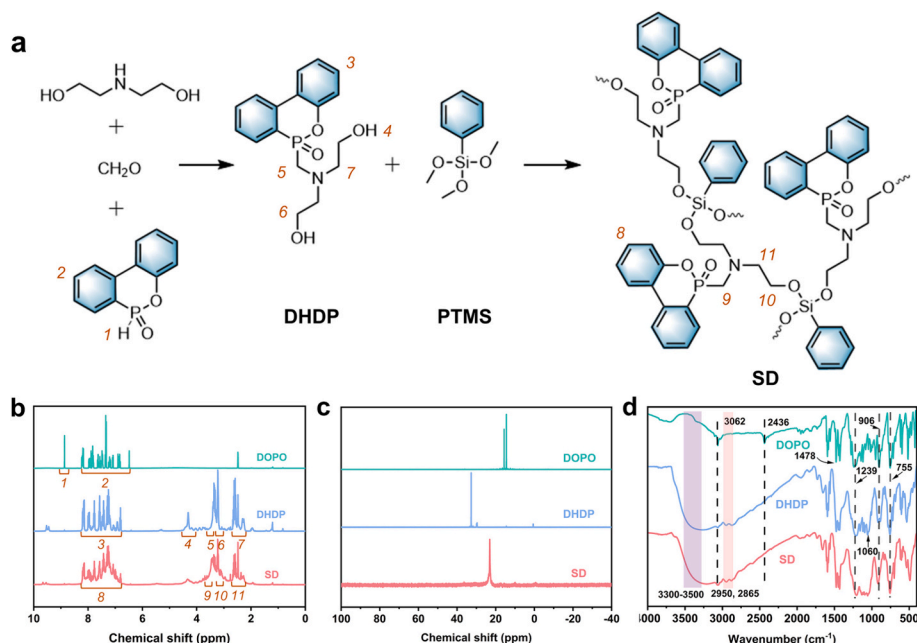This section is presented in the Supporting Information.



**Fig. 1.** (a) Synthesis route of SD; and (b) $^1$H NMR, (c) $^{31}$P NMR, and (d) FTIR spectra of DOPO, DHDP, and SD.

## 3. Results and discussion

### 3.1. Characterization of SD

SD was synthesized by two steps (see Fig. 1a): (i) the phosphorus-derived intermediate (DHDP) was synthesized by the reaction of DOPO, formaldehyde, and diethanolamine; and (ii) the final SD was synthesized using DHDP and PTMS. The chemical structure of SD was characterized by $^1$H and $^{31}$P nuclear magnetic resonance (NMR), Fourier-transform infrared spectroscopy (FTIR), and gel permeation chromatography (GPC) in Fig. 1b-d and S1. In the $^1$H NMR of DHDP (see Fig. 1b), the signal of P—H at 8.85 ppm disappears, and those belonging to the protons of -CH$_2$- and -OH appear at 2.30–2.61, 3.2–3.35, and 4.31 ppm, respectively [22–24]. For SD, there is no signal of -OH at 4.31 ppm in its $^1$H NMR since the reaction between DHDP and PTMS. Meanwhile, the $^{31}$P NMR spectra of DHDP and SD show only one peak, which is located at 32.65 and 23.00 ppm, respectively (see Fig. 1c). These results indicate that the synthesis of SD is successful. In the FTIR spectra of DOPO (see Fig. 1d), the absorption peaks at 3062, 2436, 1478, 1239 and 755 cm$^{-1}$ belong to Ph-H, P—H, Ph-P, P—O and P-O-C structures, respectively [8,25]. In the FTIR spectra of DHDP and SD, the absorption band of -OH appears at 3300–3500 cm$^{-1}$ [26], and those of -CH$_2$- and -CH= appear at 2950 and 2865 cm$^{-1}$, respectively. The disappearance of the P—H peak at 2436 cm$^{-1}$ further confirms the successful synthesis of DHDP. For SD, the absorption peak at 1134 cm$^{-1}$ belongs to Si—O structure [27]. To further illustrate the structure of SD, the GPC test was performed (see Fig. S1). The number average molecular weight ($M_n$) of SD is 10,661 g/mol, and its polydispersion index is 2.6. All these results prove that hyperbranched SD polymer has been synthesized.

### 3.2. Superior optical properties

Epoxy resins are widely used in optical fields due to their high transparency. Therefore, the effects of SD on the optical properties of EP were analyzed by UV–vis spectrophotometer and digital camera (see Fig. 2). In Fig. 2a, the transmittance of EP, EP-SD$_1$, EP-SD$_{1.5}$, EP-SD$_3$ and EP-SD$_6$ at wavelength of 900 nm is 84.8 %, 79.8 %, 81.4 %, 83.5 %, and 84.4 %, respectively, demonstrating that the addition of SD only slightly reduces the transmittance of EP. With increasing SD content, the transmission of EP film gradually increases. The ultraviolet protection factor (UPF) values of EP and EP-SD films were calculated to determine the effect of SD on the UV protection. As shown in Fig. 2b, the UPF of EP is 119.1, while that of EP-SD$_6$ is increased to 312.8, which proves that the addition of SD improves the UV-shielding function of EP. This improvement in UV protection is attributed to the UV absorption by the diphenyl groups of SD. Fig. 2d shows the digital photos of EP samples. Due to the addition of SD, the EP-SD films become darker than the EP

film, but they still maintain high transparency. These images also confirm that SD can be uniformly dispersed in the EP matrix, which is crucial for flame retardancy and mechanical properties [28].

XRD was used to study the non-crystalline structures of EP and EP-SD samples (see Fig. 2c). All samples only show a wide diffraction peak at $2\theta = 18°$ with no crystallization peak, indicating that the addition of SD does not affect the non-crystalline structure of EP, thus retaining high transparency. All these results show that EP-SD samples have high visible light transmittance and enhanced UV-shielding function.

### 3.3. Outstanding mechanical properties

Dynamic and static mechanical experiments were conducted to study the effects of SD on the mechanical properties of EP (see Fig. 3 and Table S2). With increasing SD content, the storage modulus at 25 °C increases, and finally reaches 2873 MPa for EP-SD$_6$, with a 14.1 % increase compared to that of EP. The results indicate that the introduction of SD contributes to enhancing the stiffness of EP. In Fig. 3b and Table S2, the glass transition temperature ($T_g$) of epoxy thermoset decreases as the SD loading level increases, demonstrating the decrease of cross-linking density. Meanwhile, the intramolecular cavities within SD are also responsible for the decreased $T_g$, since they increase the movement of EP chain segment [4,29].

The static mechanical properties of EP and EP-SD are shown in Fig. 3c-f and Table S2. The tensile strength and elongation at the break of EP are 53.0 MPa and 5.7 %, as shown in Fig. 3c. The introduction of SD allows EP-SD samples to achieve obviously enhance mechanical performances. Especially, the tensile strength and elongation at the break of EP-SD$_6$ are up to 90.3 MPa and 9.6 %, which are 70.4 % and 68.4 % higher than those of EP. The improved mechanical performances of EP-SD samples can also be demonstrated by their increased flexural moduli and strengths in Fig. 3d and e. The flexural strength and modulus of EP are 92.5 MPa and 2.71 GPa, while those of EP-SD$_6$ increase to 120.4 MPa and 3.06 GPa. The impact strengths of EP samples are presented in Fig. 3f, in which the impact strength of EP-SD$_6$ reaches 11.5 kJ/m$^2$, with a 59.7 % enhancement relative to 7.2 kJ/m$^2$ of EP. In general, SD simultaneously improves the stiffness, strength and toughness of EP. The flexible chain segment of SD containing methylene and Si—O is responsible for its strengthening and toughening effects. Meanwhile, the decrease of cross-linking density is beneficial to the dissipation of fracture energy under external forces, thus improving the toughness.

To study the toughening mechanism of SD, the impact fracture surfaces of EP and EP-SD samples were studied by scanning electron microscopy (SEM). In Fig. 3g$_1$-g$_2$, EP exhibits typical brittle fracture characteristics with regular surface structure, demonstrating poor toughness. On the fractured surface of EP-SD$_3$, many micro-cracks and shear bands can be observed, and their formation results in energy
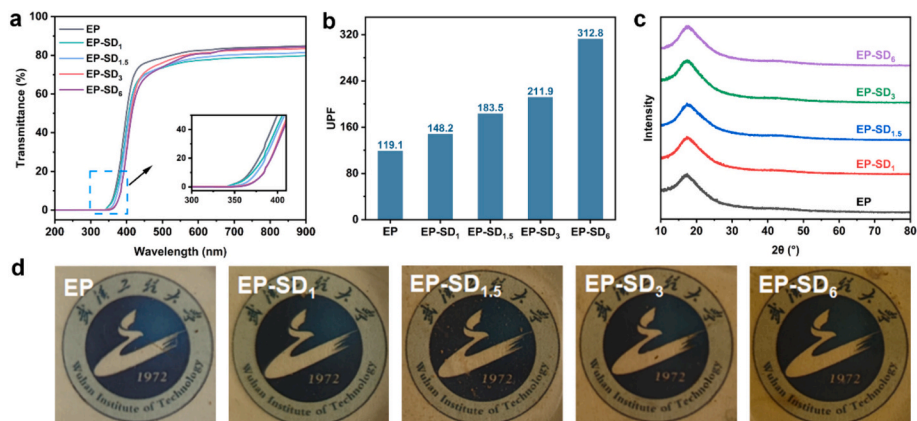


**Fig. 2.** (a) UV–visible transmission spectra, (b) UPF values, (c) XRD patterns, and (d) digital photos of EP and EP-SD films.
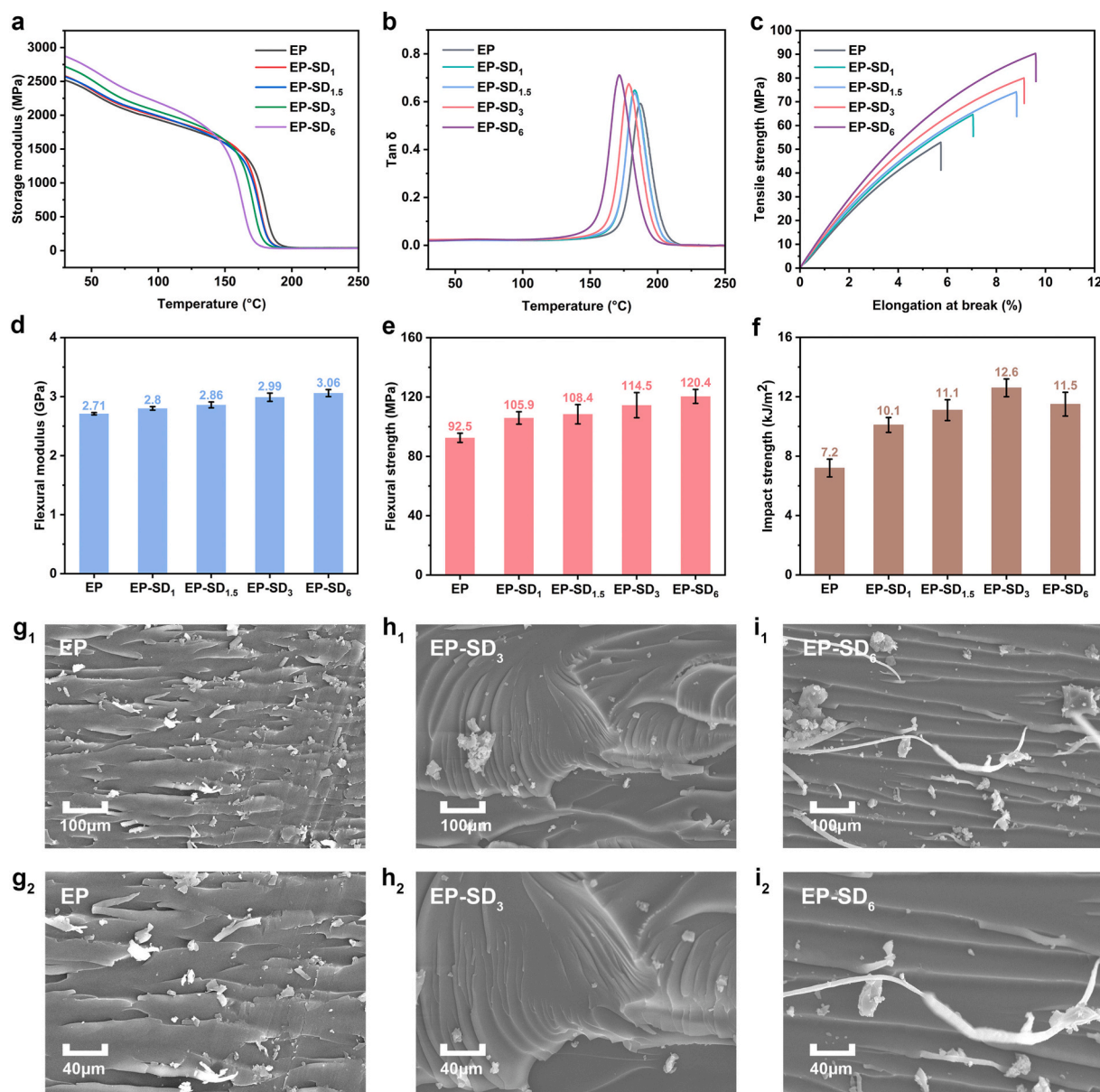
**Fig. 3.** (a) Storage modulus plots, (b) tan delta curves, (c) tensile stress-strain curves, (d) flexural moduli, (e) flexural strengths, and (f) impact strengths of EP samples; and SEM images of the cross-sections for (g$_1$, g$_2$) EP, (h$_1$, h$_2$) EP-SD$_3$, and (i$_1$, i$_2$) EP-SD$_6$ after impact tests under different magnifications.

dissipation, thereby improving toughness. There are many profilamentous structures within the cross-section of EP-SD$_6$, which are also beneficial to toughness enhancement.

### 3.4. Maintained thermal stability

The thermal stability of SD and EP samples was measured by thermogravimetric analysis (TGA) in air and N$_2$ conditions, respectively. The TG and derivative TG (DTG) curves and thermal characteristic data are shown in Fig. S2 and Table S3. The initial decomposition temperature ($T_{5\%}$: temperature at 5 wt% weight loss) values of SD are 248 and 261 °C under N$_2$ and air atmosphere, respectively, and both are much higher than the curing temperature of EP-SD. In addition, the char yield at 800 °C (CY) values of SD reach 14.0 % and 15.6 % in N$_2$ and air conditions, confirming its great carbonization performances. Under nitrogen atmosphere, all EP samples undergo one decomposition stage, which is related to the breakdown of the crosslinking network. In air conditions, there are two decomposition stages for all EP samples,

including the destruction of the network, and the further degradation of residual chars. After the addition of SD, the $T_{5\%}$ values of EP-SD samples are lower than those of EP, but their temperature at maximum weight loss rate ($T_{\max}$) values are very close. The reduced $T_{5\%}$ of EP-SD may be due to the catalytic decomposition of the phosphate-containing groups produced by the degradation of SD [30,31]. Notably, the EP-SD samples show obviously increased CY values relative to those of EP sample, indicative of enhanced char-forming ability due to the addition of SD [32].

### 3.5. Outstanding fire safety

The flame retardancy of EP and EP-SD samples was characterized by LOI and UL-94 tests (see Table S4). EP has a LOI of 26.5 % and no rating (NR) in the UL-94 test, which indicates that it is highly flammable. With the addition of SD, the LOI value and UL-94 rating of the EP-SD sample improve significantly, with the UL-94 rating reaching V-0 after adding 1.5 wt% SD, and the LOI value reaching 36.0 % after introducing 6 wt%

SD. All these results indicate that SD can endow EP with great flame retardancy at a low addition amount.

The combustion behaviors of EP and EP-SD samples were studied by cone calorimetry, with the results shown in Fig. 4 and Table S5. It is obvious that the time to ignition (TTI) of the EP-SD sample is higher than that of EP, which indicates that the initial decomposition products of SD can inhibit the ignition of the EP matrix. In addition, the PHRR and total heat release (THR) of the EP-SD thermoset are significantly reduced with the introduction of SD (see Fig. 4a and b), and especially the PHRR and THR of EP-SD$_6$ is decreased by 65.4 % and 52.7 % compared to those of EP, respectively (see Fig. 4d). Hence, the thermal degradation fragments of SD retard the heat release of the EP matrix, bring about the enhanced flame retardancy.

During the combustion process, a large amount of smoke and toxic volatile will be generated along with the heat release, and smoke is the main cause of fire casualties [33]. As can be seen from Fig. 4c and Table S5, both total smoke production (TSP) and PSPR of EP-SD significantly decrease compared to those of EP. For instance, the EP-SD$_3$ sample exhibits 41.4 % and 31.5 % reductions in TSP and PSPR (see Fig. 4e). Besides flame retardancy, SD effectively improves the smoke suppression of EP. The mechanical and flame-retardant performances of EP-SD$_6$ and previously-reported epoxy systems with the UL-94 V-0 classification [34–43] are compared in Fig. 4f. Obviously, our EP-SD$_6$

sample show much higher tensile strength increase and PHRR reduction than previous systems, further verifying its superior mechanical and flame-retardant performances. The digital photos of the char residues for EP samples are presented in Fig. 4g. EP-SD samples left more char residues than EP after cone calorimetry tests, contributing to reducing smoke release. Moreover, the integrality of the EP-SD char residues is better than that of the EP residue, so they can serve as protective layers to suppress the release of heat and smoke during combustion. In Table S5, the average effective heat of combustion (AEHC) of the EP-SD sample shows a downward trend as the SD content increases. It indicates that the decomposition products of SD can also function in gaseous phase to suppress the burning of the volatile matter. Thereby, SD can remarkably enhance both fire retardancy and smoke suppression of EP by its gas/condensed-phase functions.

### 3.6. Obvious flame-retardant action

#### 3.6.1. Condensed phase

The char microtopography of EP, EP-SD$_3$, and EP-SD$_6$ after the cone calorimetry tests was observed by SEM (see Fig. 5). In Fig. 5a$_1$ and a$_2$, both cracks and holes can be easily found on the surface of the EP char, which are not conducive to preventing heat transfer and smoke release. After the addition of 3 wt% SD, the char structure of EP-SD$_3$ significantly
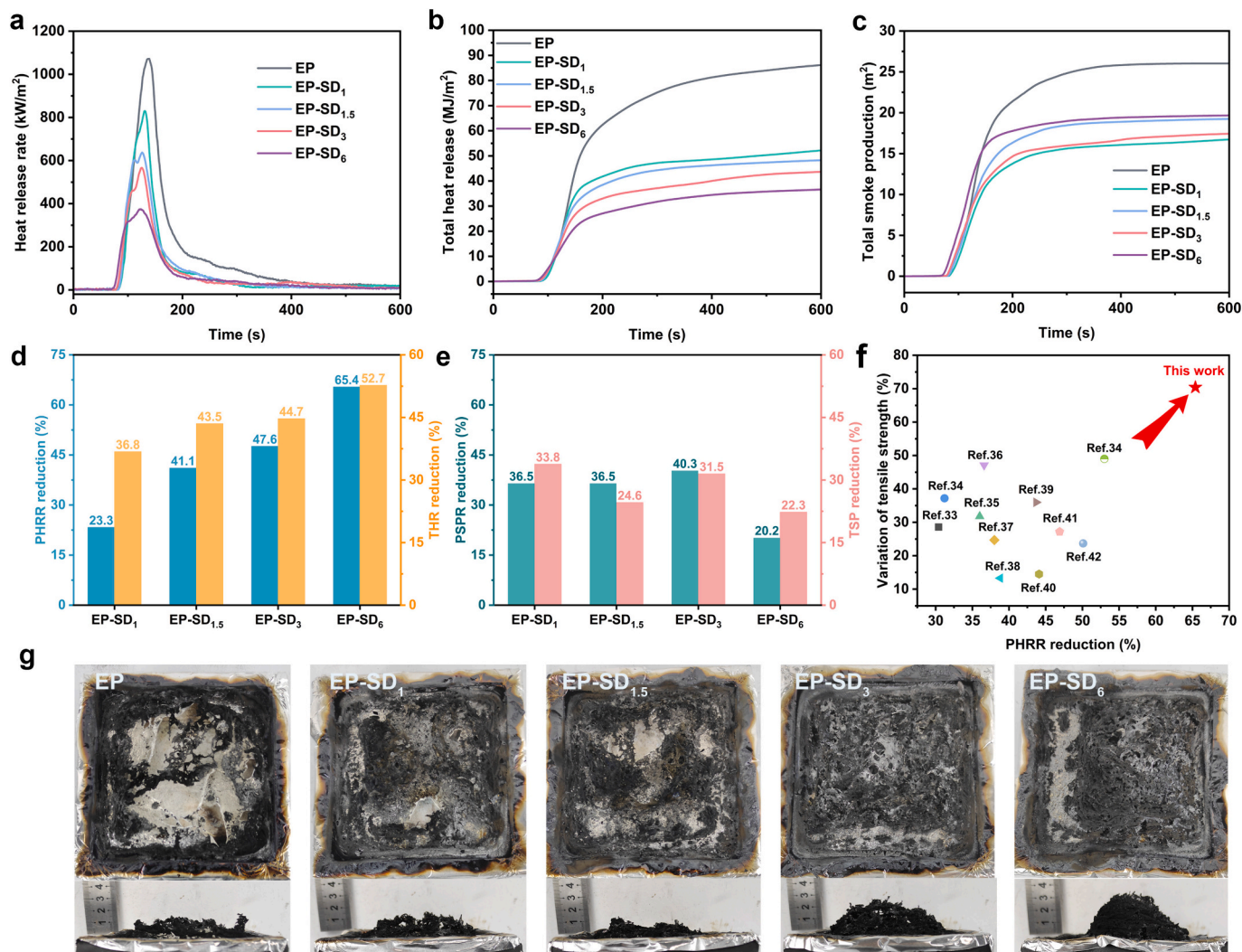


**Fig. 4.** (a) Heat release rate plots, (b) total heat release curves, (c) total smoke production curves, (d) PHRR and THR reductions, and (e) PSPR and TSP decreases of EP samples; (f) variation in tensile strength and PHRR reduction of EP-SD$_6$ and previously-reported EP samples with the UL-94 V-0 rating; and (g) top/side-view digital images of the residual chars for EP samples after cone calorimetry tests.
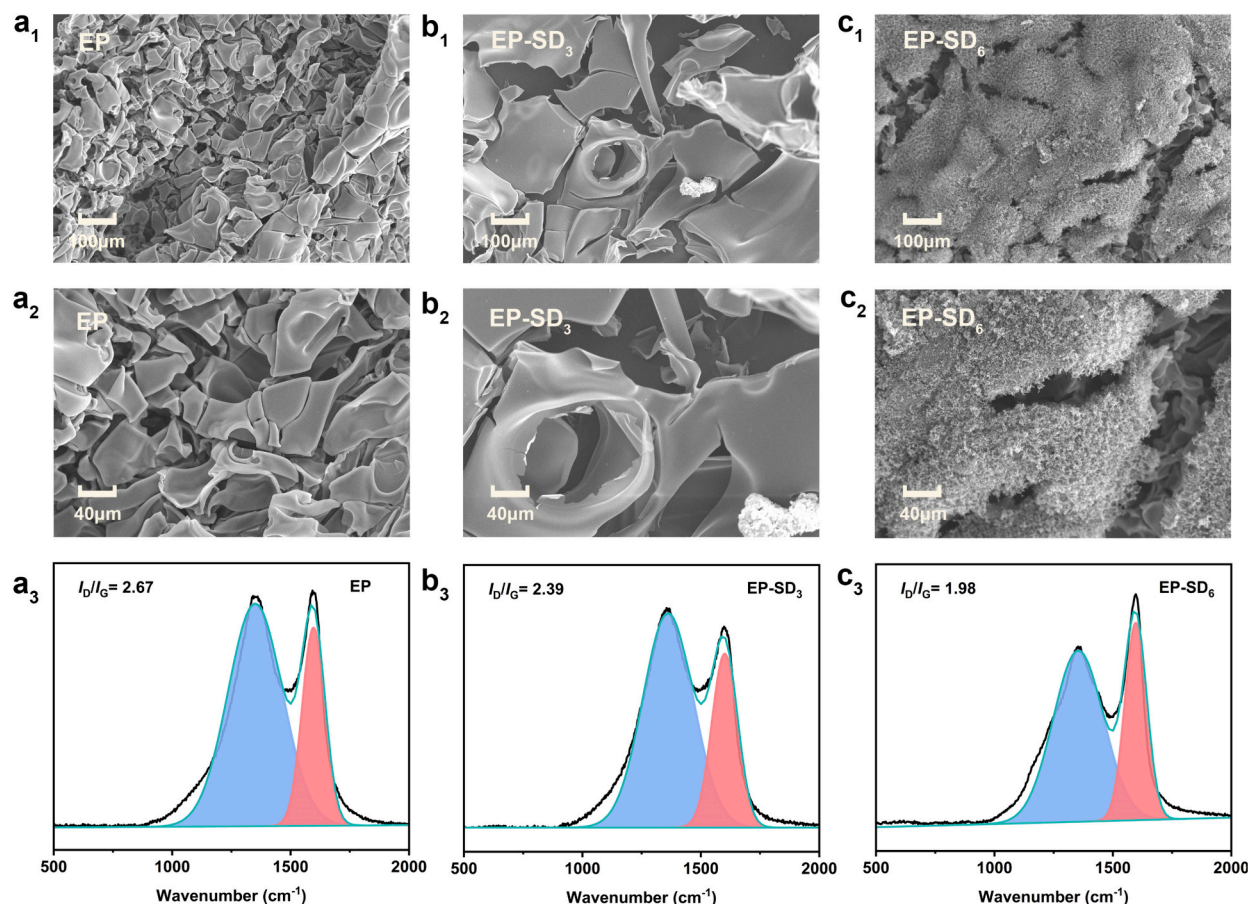
**Fig. 5.** SEM images and Raman spectra of the residual chars for (a) EP, (b) EP-SD$_3$, and (c) EP-SD$_6$ after cone calorimetry tests.

improves, and the cracks and pores are greatly reduced (see Fig. 5b$_1$ and b$_2$). Moreover, the compactness of the EP-SD$_6$ char is better than that of the EP and EP-SD$_3$ chars (see Fig. 5c$_1$ and c$_2$), further proving the condensed-phase action of SD.

The graphitization of chars was studied by laser Raman spectrometry, with the spectra displayed in Fig. 5a$_3$-c$_3$. All the residues show *D* peak and G peak at 1360 and 1605 cm$^{-1}$, respectively, in their Raman spectra, where D band belongs to a disordered carbon structure [44], and G band corresponds to a graphitized structure [32]. The area ratio of D peak to G peak ($I_D/I_G$) is inversely proportional to the char graphitization degree [45]. With increasing addition of SD, the $I_D/I_G$ value of EP-SD char monotonically reduces, and finally reaches 1.98 for EP-SD$_6$ char, indicating that SD not only promotes the carbonization of the EP matrix, but also enhances the graphitization of the char. Therefore, the condensed-phase flame-retardant action of SD is mainly reflected in its promotion of char formation and improvement of the char layer structure.

### 3.6.2. Gaseous phase

Thermogravimetric analysis/infrared spectrometry (TG-IR) tests were performed on EP and EP-SD$_3$ under nitrogen atmosphere to study the gas-phase action of SD (see Fig. 6a-c). In Fig. 6a and b, the EP and EP-SD$_3$ samples exhibit similar decomposition gas products, including water (3650 cm$^{-1}$), hydrocarbons (2975 cm$^{-1}$), carbon dioxide (2374 cm$^{-1}$), carbon monoxide (1770 cm$^{-1}$), aromatic compounds (1515 cm$^{-1}$), C-N-based organics (1257 cm$^{-1}$) and ethers (1175 cm$^{-1}$). Notably, the peak intensity of aromatic compounds, and carbon dioxide of EP-SD$_3$ is significantly lower than that of EP (see Fig. 6c$_2$ and c$_3$), indicating that the decomposition products of SD promote the carbonization of the matrix and retard the generation of pyrolysis products. In

addition, the peak intensity of EP-SD$_3$ at 747 cm$^{-1}$ is higher than that of EP (see Fig. 6c$_1$), which may be due to the release of abundant NH$_3$ gases from the degradation of SD. The NH$_3$ gases may exert diluting effect during combustion. All these results further demonstrate the promoting carbonization effect of SD.

The pyrolysis behaviors of SD were studied by pyrolysis-gas chromatography/mass spectrometry (Py-GC/MS), with results displayed in Fig. 6d and e. In the initial pyrolysis stage, the benzene fragment (m/z = 78) can be detected, which may be derived from PTMS part in SD. Then, a series of DOPO-derived fragments (m/z = 154, 166, 170, 198, and 216) are released, indicative of the pyrolysis of the DOPO part. Obviously, the release of these fragments may be accompanied by the generation of the P-containing radicals, which can quench the high-energy radicals from the EP matrix during combustion, thus suppressing the burning reaction in gas phase.

Based on the above results, the possible actions of SD in the combustion process are shown in Fig. 7: (i) The P- and N-containing radicals/fragments generated by the pyrolysis of SD quench and dilute the active radicals derived from epoxy matrix, thus inhibiting the gas-phase combustion chain reaction; and (ii) Phosphorus- and silicon-containing decomposition products of SD promote the formation of dense, expanded chars layers on the matrix surface, inhibiting the heat transfer and smoke generation. Therefore, SD plays a flame-retardant role in both condensed and gaseous phases.

## 4. Conclusions

In this work, a hyperbranched flame retardant SD containing P, N, and Si was successfully synthesized for the manufacture of high-performance, flame-retardant EP systems. SD simultaneously improves
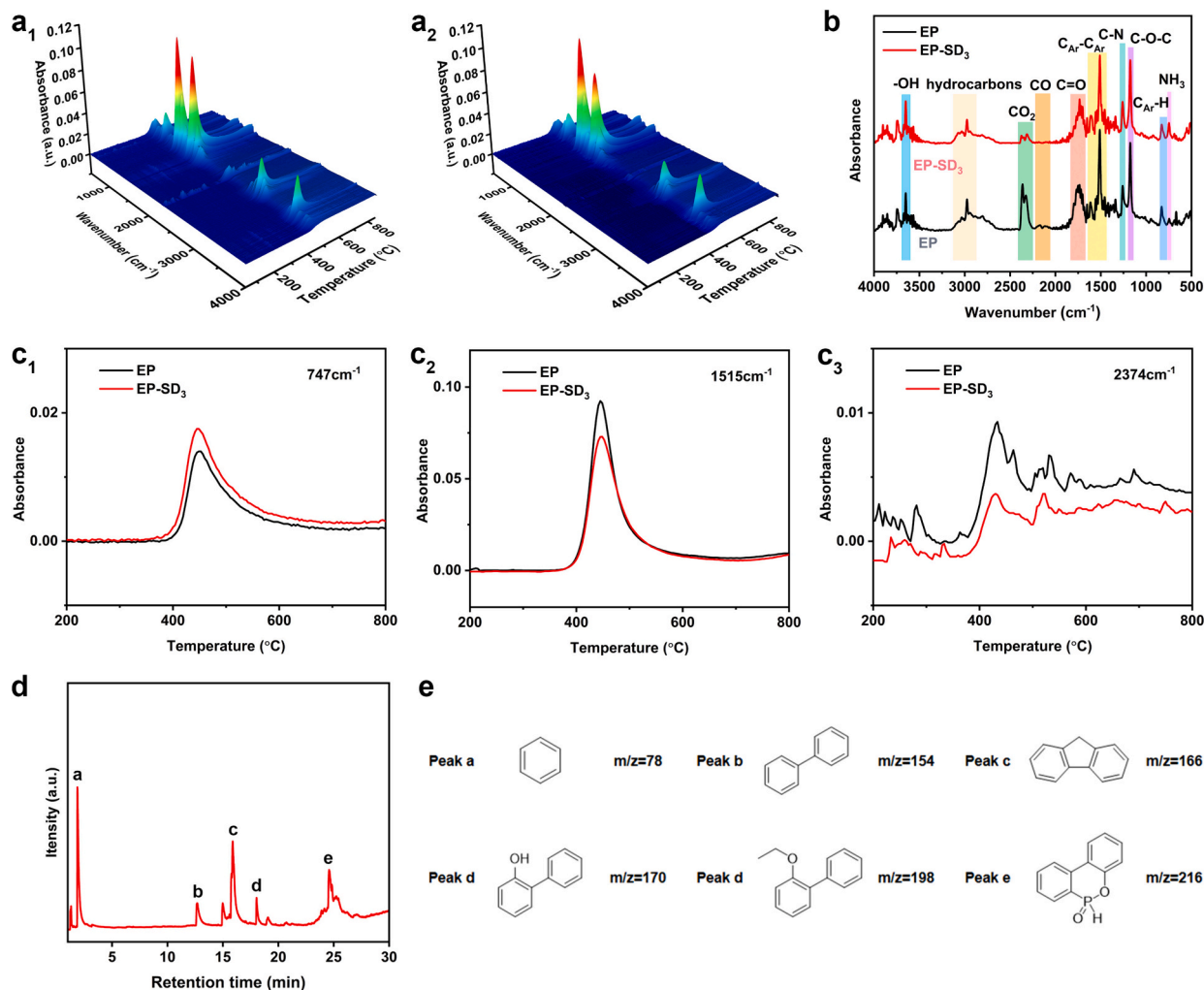
**Fig. 6.** 3D FTIR spectra of the pyrolysis products of (a₁) EP and (a₂) EP-SD₃; (b) FTIR spectra of the pyrolysis products of EP and EP-SD₃ at $T_{max}$; absorbance *vs.* temperature plots of EP and EP-SD₃ at (c₁) 747, (c₂) 1515, and (c₃) 2374 cm⁻¹; (d) total ion chromatogram of SD; and (e) the characteristic fragment structures identified from the Py-GC/MS spectra of SD.
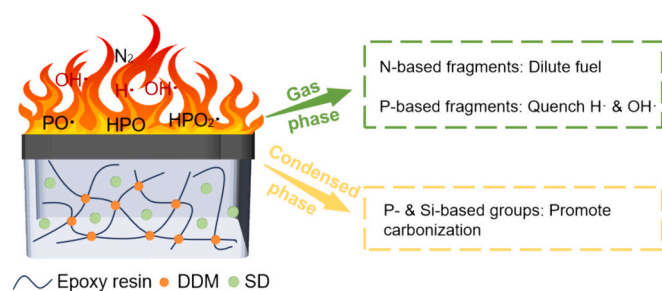


**Fig. 7.** The probable flame-retardant action of SD.

the anti-UV ability, mechanical properties, flame retardancy and smoke suppression of EP at a low addition. EP-SD₆ with 6 wt% SD shows a LOI value of 36.0 % and an UL-94 V-0 rating, with 65.4 %, 52.7 %, 20.2 % and 22.3 % reductions in PHRR, THR, PSPR and TSP relative to those of EP. The superior fire retardancy and smoke suppression of EP-SD₆ are mainly due to the combined action of the P, N, and Si elements in SD. Additionally, compared with EP, the UPF of EP-SD₆ increases by 162.6 %, and tensile strength, elongation at break, flexural strength and impact strength increase by 70.4 %, 40.6 %, 30.2 % and 59.7 %, respectively. Obviously, the outstanding comprehensive performances of EP-SD₆ enable it to outperform previously-reported flame-retardant

epoxy systems. This work provides an integrated and effective strategy for preparing fire-retardant and smoke-suppressive EP thermosets with great optical and mechanical properties.

**CRediT authorship contribution statement**

**Siqi Huo:** Writing – review & editing, Project administration, Funding acquisition, Conceptualization. **Cheng Wang:** Formal analysis. **Guofeng Ye:** Investigation. **Qi Zhang:** Validation, Conceptualization. **Pingan Song:** Formal analysis. **Hao Wang:** Writing – original draft, Investigation. **Zhitian Liu:** Supervision, Project administration.

**Declaration of competing interest**

The authors declare that they have no known competing financial interests or personal relationships that could have appeared to influence the work reported in this paper.

**Data availability**

Data will be made available on request.

## Appendix A. Supplementary data

Supplementary data to this article can be found online at https://doi.org/10.1016/j.porgcoat.2024.108562.

## References

[1] M. Chen, X. Lin, C. Liu, H. Zhang, An effective strategy to enhance the flame retardancy and mechanical properties of epoxy resin by using hyperbranched flame retardant, J. Mater. Sci. 56 (9) (2021) 5956–5974, https://doi.org/10.1007/s10853-020-05691-3.

[2] X. Mi, N. Liang, H. Xu, J. Wu, Y. Jiang, B. Nie, D. Zhang, Toughness and its mechanisms in epoxy resins, Prog. Mater. Sci. 130 (2022) 100977, https://doi.org/10.1016/j.pmatsci.2022.100977.

[3] C. Wang, S. Huo, G. Ye, B. Wang, Z. Guo, Q. Zhang, P. Song, H. Wang, Z. Liu, Construction of an epoxidized, phosphorus-based poly(styrene butadiene styrene) and its application in high-performance epoxy resin, Compos. Part B 268 (2024) 111075, https://doi.org/10.1016/j.compositesb.2023.111075.

[4] G. Ye, S. Huo, C. Wang, Q. Shi, L. Yu, Z. Liu, Z. Fang, H. Wang, A novel hyperbranched phosphorus-boron polymer for transparent, flame-retardant, smoke-suppressive, robust yet tough epoxy resins, Compos. Part B 227 (2021) 109395, https://doi.org/10.1016/j.compositesb.2021.109395.

[5] S. Huo, T. Sai, S. Ran, Z. Guo, Z. Fang, P. Song, H. Wang, A hyperbranched P/N/B-containing oligomer as multifunctional flame retardant for epoxy resins, Compos. Part B 234 (2022) 109701, https://doi.org/10.1016/j.compositesb.2022.109701.

[6] D. Liu, Y. Cui, T. Zhang, W. Zhao, P. Ji, Improving the flame retardancy and smoke suppression of epoxy resins by introducing of DOPO derivative functionalized ZIF-8, Polym. Degrad. Stab. 194 (2021) 109749, https://doi.org/10.1016/j.polymdegradstab.2021.109749.

[7] J. Kamalipour, M.H. Beheshty, M.J. Zohuriaan-Mehr, Novel phosphonated hardeners derived from diamino diphenyl sulfone for epoxy resins: synthesis and one-pack flame-retardant formulation alongside dicyandiamide, Polym. Degrad. Stab. 199 (2022) 109917, https://doi.org/10.1016/j.polymdegradstab.2022.109917.

[8] H. Wang, J. Yuan, Y. Wang, Y. Ma, S. Lyu, Z. Zhu, A nitrogen heterocyclic/phosphaphenanthrene derivative as a reactive additive for simultaneous improvement of flame retardancy, mechanical and dielectric properties of epoxy resins, Polym. Degrad. Stab. 199 (2022) 109909, https://doi.org/10.1016/j.polymdegradstab.2022.109909.

[9] W. Wang, Y. Liu, H. Wen, Q. Wang, Synthesis of a hyperbranched polyamide charring agent and its flame-retarding and toughening behavior in epoxy resin, Polym. Degrad. Stab. 184 (2021) 109479, https://doi.org/10.1016/j.polymdegradstab.2020.109479.

[10] P. Wang, L. Chen, H. Xiao, T. Zhan, Nitrogen/sulfur-containing DOPO based oligomer for highly efficient flame-retardant epoxy resin, Polym. Degrad. Stab. 171 (2020) 109023, https://doi.org/10.1016/j.polymdegradstab.2019.109023.

[11] S. Huo, J. Wang, S. Yang, H. Cai, B. Zhang, X. Chen, Q. Wu, L. Yang, Synergistic effect between a novel triazine-based flame retardant and DOPO/HPCP on epoxy resin, Polym. Adv. Technol. 29 (11) (2018) 2774–2783, https://doi.org/10.1002/pat.4400.

[12] S. Huo, J. Wang, S. Yang, J. Wang, B. Zhang, B. Zhang, X. Chen, Y. Tang, Synthesis of a novel phosphorus-nitrogen type flame retardant composed of maleimide, triazine-trione, and phosphaphenanthrene and its flame retardant effect on epoxy resin, Polym. Degrad. Stab. 131 (2016) 106–113, https://doi.org/10.1016/j.polymdegradstab.2016.07.013.

[13] W. He, P. Song, B. Yu, Z. Fang, H. Wang, Flame retardant polymeric nanocomposites through the combination of nanomaterials and conventional flame retardants, Prog. Mater. Sci. 114 (2020) 100687, https://doi.org/10.1016/j.pmatsci.2020.100687.

[14] J.-H. Lu, Y.-J. Xu, L. Chen, J.-H. Chen, J.-H. He, Z. Li, S.-L. Li, Y.-Z. Wang, Facile fabrication of intrinsically fire-safety epoxy resin cured with phosphorus-containing transition metal complexes for flame retardation, smoke suppression, and latent curing behavior, Chem. Eng. J. 442 (2022) 136097, https://doi.org/10.1016/j.cej.2022.136097.

[15] Y. Zhang, B. Yu, B. Wang, K.M. Liew, L. Song, C. Wang, Y. Hu, Highly effective P–P synergy of a novel DOPO-based flame retardant for epoxy resin, Ind. Eng. Chem. Res. 56 (5) (2017) 1245–1255, https://doi.org/10.1021/acs.iecr.6b04292.

[16] X. Wu, H. Zhu, W. Xi, Y. Qiu, J. Li, L. Qian, Esterification oligomerization of phosphaphenanthrene biphenol caused efficient flame retardant effect of group aggregation in epoxy resin, ACS Appl. Polym. Mater. 5 (5) (2023) 3381–3388, https://doi.org/10.1021/acsapm.3c00053.

[17] Q. Shi, S. Huo, C. Wang, G. Ye, L. Yu, Z. Fang, H. Wang, Z. Liu, A phosphorus/silicon-based, hyperbranched polymer for high-performance, fire-safe, transparent epoxy resins, Polym. Degrad. Stab. 203 (2022) 110065, https://doi.org/10.1016/j.polymdegradstab.2022.110065.

[18] M. Fang, J. Qian, X. Wang, Z. Chen, R. Guo, Y. Shi, Synthesis of a novel flame retardant containing phosphorus, nitrogen, and silicon and its application in epoxy resin, ACS Omega 6 (10) (2021) 7094–7105, https://doi.org/10.1021/acsomega.1c00076.

[19] N. Teng, J. Dai, S. Wang, J. Hu, X. Liu, Hyperbranched flame retardant for epoxy resin modification: simultaneously improved flame retardancy, toughness and strength as well as glass transition temperature, Chem. Eng. J. 428 (2022) 131226, https://doi.org/10.1016/j.cej.2021.131226.

[20] J.X. Cheng, W.A. Cai, Z.C. Wang, A.Q. Dayo, Z.G. Yuan, W.B. Liu, J. Wang, Z.C. Pan, Synthesis of a novel boron-containing hyperbranched benzoxazine and its flame-retardant properties in copolymer with epoxy resin, Polym. Adv. Technol. 34 (8) (2023) 2694–2706, https://doi.org/10.1002/pat.6083.

[21] X. Chen, F. Peng, C. Wang, H. Zhou, X. Lin, W. Liu, A. Zhang, Improving the flame retardancy and mechanical properties of epoxy composites significantly with a low-loading CNT-based hierarchical hybrid decorated with reactive hyperbranched polyphosphoramide, Appl. Surf. Sci. 576 (2022) 151765, https://doi.org/10.1016/j.apsusc.2021.151765.

[22] Z. Chi, Z. Guo, Z. Xu, M. Zhang, M. Li, L. Shang, Y. Ao, A DOPO-based phosphorus-nitrogen flame retardant bio-based epoxy resin from diphenolic acid: synthesis, flame-retardant behavior and mechanism, Polym. Degrad. Stab. 176 (2020) 109151, https://doi.org/10.1016/j.polymdegradstab.2020.109151.

[23] L. Gao, G. Zheng, X. Nie, Y. Wang, Thermal performance, mechanical property and fire behavior of epoxy thermoset based on reactive phosphorus-containing epoxy monomer, J. Therm. Anal. Calorim. 127 (2) (2016) 1419–1430, https://doi.org/10.1007/s10973-016-5456-0.

[24] C. Wang, S. Huo, G. Ye, P. Song, H. Wang, Z. Liu, A P/Si-containing polyethylenimine curing agent towards transparent, durable fire-safe, mechanically-robust and tough epoxy resins, Chem. Eng. J. 451 (2023) 138768, https://doi.org/10.1016/j.cej.2022.138768.

[25] S. Huo, Z. Liu, C. Li, X. Wang, H. Cai, J. Wang, Synthesis of a phosphaphenanthrene/benzimidazole-based curing agent and its application in flame-retardant epoxy resin, Polym. Degrad. Stab. 163 (2019) 100–109, https://doi.org/10.1016/j.polymdegradstab.2019.03.003.

[26] J. Hu, L. Zhang, M. Chen, J. Dai, N. Teng, H. Zhao, X. Ba, X. Liu, Synthesis of hyperbranched flame retardants with varied branched chains' rigidity and performance of modified epoxy resins, Polymers 15 (2) (2023), https://doi.org/10.3390/polym15020449.

[27] H. Qiao, M. Chen, B. Chen, H. Zhang, B. Zheng, Understanding the curing kinetics of boron-based hyperbranched polysiloxane reinforced and toughened epoxy resin by rheology, Chem. Eng. J. 467 (2023) 143542, https://doi.org/10.1016/j.cej.2023.143542.

[28] T. Sai, S. Ran, Z. Guo, H. Yan, Y. Zhang, H. Wang, P. Song, Z. Fang, Transparent, highly thermostable and flame retardant polycarbonate enabled by rod-like phosphorous-containing metal complex aggregates, Chem. Eng. J. 409 (2021) 128223, https://doi.org/10.1016/j.cej.2020.128223.

[29] D. Foix, X. Ramis, F. Ferrando, A. Serra, Improvement of epoxy thermosets using a thiol-ene based polyester hyperbranched polymer as modifier, Polym. Int. 61 (5) (2012) 727–734, https://doi.org/10.1002/pi.3230.

[30] X. Peng, Z. Li, D. Wang, Z. Li, C. Liu, R. Wang, L. Jiang, Q. Liu, P. Zheng, A facile crosslinking strategy endows the traditional additive flame retardant with enormous flame retardancy improvement, Chem. Eng. J. 424 (2021) 130404, https://doi.org/10.1016/j.cej.2021.130404.

[31] X. Peng, Q. Liu, D. Wang, C. Liu, Y. Zhao, R. Wang, P. Zheng, A hyperbranched structure formed by in-situ crosslinking of additive flame retardant endows epoxy resins with great flame retardancy improvement, Compos. Part B 224 (2021) 109162, https://doi.org/10.1016/j.compositesb.2021.109162.

[32] G. Ye, S. Huo, C. Wang, P. Song, Z. Fang, H. Wang, Z. Liu, Durable flame-retardant, strong and tough epoxy resins with well-preserved thermal and optical properties via introducing a bio-based, phosphorus-phosphorus, hyperbranched oligomer, Polym. Degrad. Stab. 207 (2023) 110235, https://doi.org/10.1016/j.polymdegradstab.2022.110235.

[33] J. Wang, J. Wang, S. Yang, K. Chen, Single-component flame-retardant and smoke-suppressive epoxy resins enabled by an aluminum/phosphorus/imidazole-containing complex, Compos. Part B 253 (2023) 110571, https://doi.org/10.1016/j.compositesb.2023.110571.

[34] G. Hu, X. Zhang, M. Bu, C. Lei, Toughening and strengthening epoxy resins with a new bi-DOPO biphenyl reactive flame retardant, Eur. Polym. J. 178 (2022) 111488, https://doi.org/10.1016/j.eurpolymj.2022.111488.

[35] J. Zhang, H. Duan, J. Zou, J. Cao, C. Wan, C. Zhang, H. Ma, A DOPO derivative constructed by sulfaguanidine and thiophene toward enhancing fire safety, smoke suppression, and mechanical properties of epoxy resin, Macromol. Mater. Eng. 306 (12) (2021) 2100569, https://doi.org/10.1002/mame.202100569.

[36] Z. Hou, H. Cai, C. Li, B. Li, H. Wang, A phosphorus/silicon/triazine-containing flame retardant towards flame retardancy and mechanical properties of epoxy resin, J. Appl. Polym. Sci. 139 (31) (2022) e52712, https://doi.org/10.1002/app.52712.

[37] W. Luo, D. Li, M. Chen, L. Su, W. Zhong, J. Lan, B. Zheng, H. Zhang, A novel polyaromatic ring phosphor-nitrogen imidazole derivative endowing epoxy resin with remarkable flame retardancy and mechanical properties, J. Polym. Res. 29 (7) (2022) 306, https://doi.org/10.1007/s10965-022-03161-9.

[38] F.Q. Pang, X.D. Liu, X.T. Zheng, Y.C. Lin, R.K. Jian, An intrinsic flame retardant epoxy resin with high transparency and strengthened mechanical property, J. Appl. Polym. Sci. 138 (42) (2021) 51230, https://doi.org/10.1002/app.51230.

[39] Y. Gao, H. Duan, J. Kang, J. Zhang, Y. Chen, W. Liu, Y. Li, A simple synthesis of a guaiacol based reactive flame retardant and its application in epoxy resins, Polym. Chem. UK (2024), https://doi.org/10.1039/d4py00051j.

[40] Y. Luo, J. Cai, L. Li, X. Lin, L. Xiao, L. Hou, Multi-DOPO-based derivative for enhancing flame retardancy and mechanical properties of epoxy resin, Prog. Org. Coat. 184 (2023) 107862, https://doi.org/10.1016/j.porgcoat.2023.107862.

[41] Y. Wang, Y. Zhang, L. Ma, H. Ge, J. Gao, Z. Zhu, Y. Weng, Facile synthesis of phosphorus-containing benzotriazole flame retardant for enhancement of mechanical and fire properties of epoxy resins, Eur. Polym. J. 202 (2024) 112610, https://doi.org/10.1016/j.eurpolymj.2023.112610.

[42] L. Zhong, T. Li, J. Zhang, J. Wang, D. Zhang, Simultaneously improving the flame retardancy and toughness of epoxy composites with hyperbranched phosphorus-containing polysiloxane functionalized halloysite nanotubes, Eur. Polym. J. 179 (2022) 111564, https://doi.org/10.1016/j.eurpolymj.2022.111564.

[43] J. Cao, H. Duan, J. Zou, J. Zhang, C. Wan, C. Zhang, H. Ma, Bio-based phosphorus-containing benzoxazine towards high fire safety, heat resistance and mechanical properties of anhydride-cured epoxy resin, Polym. Degrad. Stab. 198 (2022) 109878, https://doi.org/10.1016/j.polymdegradstab.2022.109878.

[44] S. Yang, S. Huo, J. Wang, B. Zhang, J. Wang, S. Ran, Z. Fang, P. Song, H. Wang, A highly fire-safe and smoke-suppressive single-component epoxy resin with switchable curing temperature and rapid curing rate, Compos. Part B 207 (2021) 108601, https://doi.org/10.1016/j.compositesb.2020.108601.

[45] J. Wang, X. Chen, J. Wang, S. Yang, K. Chen, L. Zhu, S. Huo, P. Song, H. Wang, High-performance, intrinsically fire-safe, single-component epoxy resins and carbon fiber reinforced epoxy composites based on two phosphorus-derived imidazoliums, Polym. Degrad. Stab. 208 (2023) 110261, https://doi.org/10.1016/j.polymdegradstab.2023.110261.